Detection of the Helium Focusing Cone in X-Rays

B.J. Wargelin, J.D. Slavin, J.C. Raymond, P.P Plucinsky, V.A. Kharchenko, M. Juda, R. Edgar, A. Dalgarno,
Harvard-Smithsonian Center for Astrophysics
and
I.P. Robertson, and T.E. Cravens
University of Kansas

Abstract

We have analyzed soft X-ray background (SXRB) data from seven Chandra observations of SN1999em in order to search for charge exchange (CX) emission from the helium focusing cone, a region on the downwind side of the Sun where the density of heliospheric neutral helium is enhanced by gravitational focusing as the Sun moves through the Local Interstellar Cloud. Six of the observations looked through the heliospheric tail where neutral gas density is low, but one of the observations looked through the He cone while the Earth was positioned inside it. This last observation (ObsID 765) reveals enhanced SXRB emission that arises from CX as highly charged solar wind ions collide with relatively dense neutral gas. We present preliminary results from a comparison of data from ObsID 765 and two other observations made when the Earth was to the side of the He cone.

Charge Exchange Emission

Solar wind charge exchange (CX) is now recognized to be a significant contributor to the observed soft X-ray background (SXRB). CX emission arises when highly charged ions in the solar wind, primarily hydrogenic and fully stripped oxygen, collide with neutral gas in the heliosphere and in Earth's extended outer atmosphere, or geocorona. During such collisions, an electron from the neutral atom is transferred to an excited energy level in the ion, from which it then radiatively decays releasing an X-ray. As seen in Figure 1, most of the emission is from He-like and H-like O at energies between 550 and 850 eV. Significant emission also comes from highly charged C ions, but primarily at energies where X-ray detector efficiency is usually low.

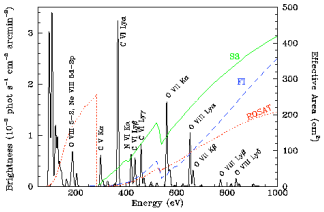

Fig. 1. Model CX spectrum, also showing effective areas of *Chandra* ACIS S3 and Front-Illuminated (FI) chips and *ROSAT* PSPC. From Wargelin et al. (2004).

Evidence for solar wind CX comes from the strong correlation of the intensity and temporal behavior of the long term enhancements (LTEs) observed by *ROSAT* and the product of the solar wind density and velocity (Cravens et al. 2001). Spectral proof comes from *Chandra* observations of the dark side of the Moon (Figure 2) and *XMM* observations of the Hubble Deep Field-North (Figure 3).

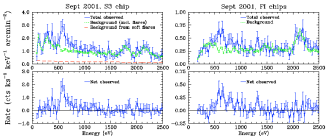

Fig. 2. *Chandra* spectra of the dark side of the Moon. Emission is completely due to geocoronal CX, with prominent He-like and H-like O lines. Weak He-like Mg emission is also visible in the FI spectrum. From Wargelin et al. (2004).

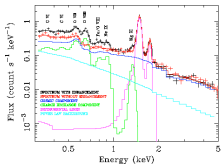

Fig. 3. *XMM* spectra of multiple observations of the HDF-N background. One observation showed a strong enhancement of CX emission (in green) from CX. From Snowden et al. (2004).

Neutral Gas and Emission Distribution

The Sun is located with the Local Interstellar Cloud (LIC), a region of partially neutral gas a few parsecs in size. As the LIC moves with respect to the Sun, H atoms and ions interact with the solar wind and magnetic field and a bow-shock forms (see Figure 4). Most of the ionized H is deflected and sweeps around the Sun but much of the neutral H streams into the heliosphere. Near the Sun, neutral H is photoionized so that it is severely depleted downwind. He atoms are less affected by the bow-shock and photoionization and are also gravitationally focused behind the Sun, creating a high density "He focusing cone" (Figure 5). Within this region, CX emission is strongly enhanced (Figure 6), particularly with respect to the low-emission region downwind where there is very little neutral H.

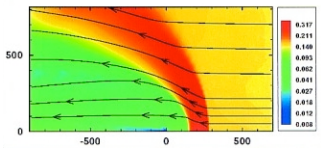

Fig. 4. Model of neutral H density around the Sun (actually, it's alpha Cen, but close enough). Axis units are in AU. Neutral H is strongly depleted downwind by photoionization as it flows by the Sun. From Wood et al. (2001).

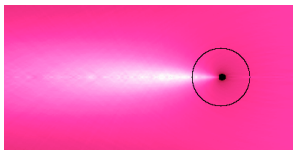

Fig. 5. Model of neutral He, which is gravitationally focused downwind of the Sun. The Earth's orbit (circle) nearly intersects the axis of the cone (angled 6 degrees below the ecliptic) each year on December 6.

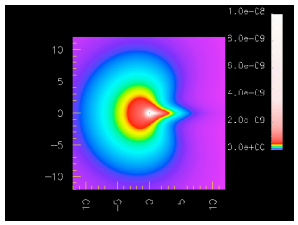

Fig. 6. Model of CX emissivity. Downwind is to the right (opposite of Figures 4 and 5). CX emissivity is proportional to the solar wind density which falls as r^{-2} so most CX emission is within a few AU of the Sun. From Pepino et al. (2004).

Observations

We searched the *Chandra* archive for multiple observations of a field lying in the approximate direction of the He cone. The best candidates were seven observations of SN1999em made between late 1999 and mid-2001 using various combinations of instrument parameters (see Table 1). This target lies in a relatively uncrowded field roughly toward the Galactic anti-center (l = 199° 33', b = -30° 01'), but unfortunately in a region of rather high SXRB emission (Figure 7). One of the observations, ObsID 765, was taken on 1999 Dec 16, when the Earth was near the densest part of the He focusing cone, looking roughly along the axis of the cone (Figures 8 and 9).

Table 1
Observation Parameters

ObsID	Exp (ks)	Date	CCDs	Mode	Array	Temp (°C)
763	25	11/01/99	I23, S234	VF	1/2	-110
764	25	11/13/99	I23, S234	VF	1/2	-110
765	35	12/16/99	I23, S234	F	full	-110
766	30	02/07/00	I23, S1234	F	full	-120
1968	30	10/30/00	I23, S1234	F	full	-120
1969	30	03/06/01	I23, S1234	F	full	-120
1970	30	07/22/01	I23, S1234	F	full	-120

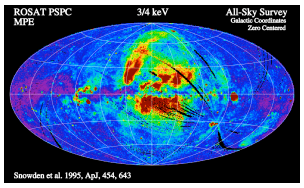

Fig. 7. Soft X-ray background measured by ROSAT in the 3/4-keV band. The field under study lies near (l,b) = (200°, -30°), as marked.

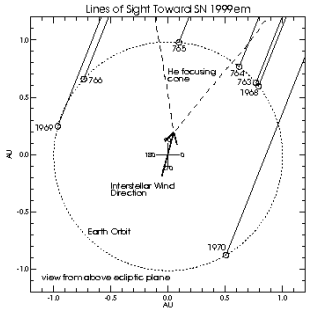

Fig. 8. Lines of sight of the seven observations of SN1999em. ObsID 765 was taken while the Earth was within the He focusing cone (rough extent as marked).

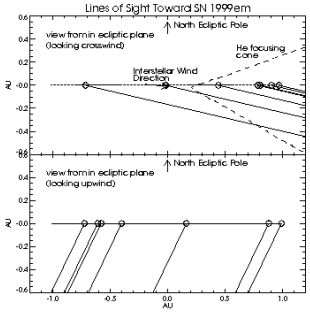

Fig. 9. Same as Figure 8 but with orthogonal views.

Because each observation had a different roll angle there is relatively little overlap in fields of view (see Figure 10); the intersection of all 7 observations is only about 1/3 of one CCD (S3). Because the SXRB can vary on scales of several arcminutes or less, it is important to compare results using exactly the same field. Preliminary results using data from the S3 CCD indicate that background emission is indeed highest in ObsID 765 and we will compare that ObsID pairwise with the other six. Here we present results from a comparison of ObsID 765 with two other observations conducted at roughly the same time of year that have very similar fields of view (FoV), ObsIDs 766 and 1969. The intersection of their FoV with 765's is shown in Figure 11. (To simplify analysis, the FoV intersection of S3 with Front-Illuminated CCDs (I2, I3, and S2) was not included.)

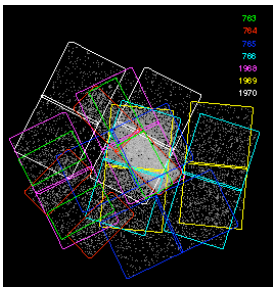

Fig. 10. Fields of view of the seven observations (excluding S4, which has an unusably high intrinsic background). The aimpoint was on S3, in the center.

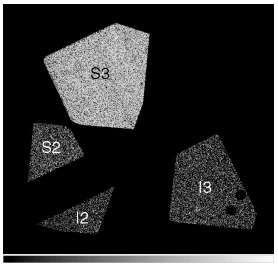

Fig. 11. FoV overlaps for ObsIDs 765, 766, and 1969, not including S2/S3 overlap. Large holes in I3 (and many smaller ones) are source exclusion regions.

Comparison of Spectra

Spectra from the S3 CCD of ObsID 765 (collected from within the He focusing cone) and ObsIDs 766+1969 (which looked through a low-neutral-density region from the "side" of the Sun) are shown in Figure 12. A significant enhancement of O line emission from CX is seen in ObsID 765. A similar enhancement is seen in the other CCDs but with poorer statistics because of their lower QE.

The observed difference corresponds to ~100×10^{-6} cts/s/arcmin^2 in the *ROSAT* 3/4-keV band, which is a typical value for the SXRB (dark blue regions in Figure 7) away from Galactic structures such as the North Polar Spur (top center arc in Figure 7). This is a clear example of how the apparent SXRB can dramatically differ from the *ROSAT* All-Sky Survey map depending on the observer's location.

Our intention is to use this and similar analyses to refine models of heliospheric CX emission (and therefore models of the SXRB and the local ISM), which currently have large uncertainties. There are also, of course, significant implications for the analysis of extended sources observed by *any* X-ray observatory.

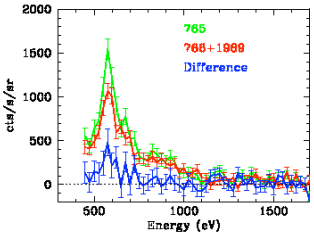

Fig. 12. Spectra from ACIS-S3 CCD, comparing ObsID 765 versus 766+1969. The difference in O line emission is due to enhanced solar wind charge exchange in the helium focusing cone downwind of the Sun, through which ObsID 765 observed.

References

Cravens, T.E., Robertson, & Snowden 2001, JGR 106, 24883
Pepino, et al. 2004, ApJ 617, 1347
Snowden, S., et al. 1995, ApJ 454, 643
Snowden, S., Collier, & Kuntz 2004, ApJ 610, 1182
Wargelin, B.J., et al. 2004, ApJ 607, 596
Wood, B.E, et al. 2001, ApJL 547, 49